JOURNAL OF MATERIALS SCIENCE: MATERIALS IN MEDICINE **16** (2005) 1069– 1075

Fabrication of polymeric scaffolds with a controlled distribution of pores

J. S. CAPES[1], H. Y. ANDO[2], R. E. CAMERON[1]
[1]*Pfizer Institute for Pharmaceutical Materials Science, Department of Materials Science and Metallurgy, University of Cambridge, Cambridge, UK*
[2]*Pfizer Inc., Pfizer Global Research and Development, Ann Arbor Laboratories, Ann Arbor, Michigan, USA*

The design of tissue engineering scaffolds must take into account many factors including successful vascularisation and the growth of cells. Research has looked at refining scaffold architecture to promote more directed growth of tissues through well-defined anisotropy in the pore structure. In many cases it is also desirable to incorporate therapeutic ingredients, such as growth factors, into the scaffold so that their release occurs as the scaffold degrades. Therefore, scaffold fabrication techniques must be found to precisely control, not only the overall porosity of scaffolds, but also the pore size, shape and spatial distribution.

This work describes the use of a regularly shaped porogen, sugar spheres, to manufacture polymeric scaffolds. Results show that pre-assembling the spheres created scaffolds with a constant porosity of 60%, but with varying pores sizes from 200–800 μm, leading to a variation in the surface area and likely degradation rate of the scaffolds. Employing different polymer impregnation techniques tailored the number of pores present with a diameter of less than 100 μm to suit different functions, and altering the packing structure of the sugar spheres created scaffolds with novel layered porosity. Replacing sugar spheres with sugar strands formed scaffolds with pores aligned in one direction.

1. Introduction

Tissue engineering can be defined as the regeneration of tissues and the restoration of functions of organs through the implantation of cells grown on an appropriate scaffold [1]. To this end, biodegradable tissue engineering scaffolds have to fulfil several functions. They must be designed in such a way as to encourage the growth of the cells. Once implanted, the scaffold must have the correct mechanical properties to match the missing tissue, and the scaffold material must then degrade in such a way as to transfer the forces to the growing tissue gradually over time.

As the primary function of the scaffold is to support the growing tissue, it must allow cell migration, attachment and proliferation. To satisfy these functions it must have a high porosity, high surface area and a specific three-dimensional shape, which can be tailored to suit the requirements of different types of tissue [2, 3].

There has been much research into the morphological design of scaffolds to promote cellular growth. Several factors are important including the pore shape and size, as well as their interconnectivity and spatial distribution through the scaffold. The scaffold architecture is crucial in allowing vascularisation and the supply of nutrients to the developing tissue. Studies have shown that pores in the region of 200 μm are required for this purpose, and that cells prefer pores with a diameter of, on average, less than 100 μm to settle and spread [4].

There are many different methods for manufacturing scaffolds, and the chosen technique is usually dependent on the properties of the material being used. Traditional methods for the formation of polymeric structures include the use of phase separation techniques [5, 6], particulate leaching [7, 8] and gas/CO_2 foaming [9–12], along with techniques for the fabrication of polymer-ceramic composites [13]. Recent research has looked at the use of alternative methods such as emulsion templating [14, 15] and solid free-forming [16, 17]. There are advantages to many of these methods such as ease of manufacture [5, 6, 9–12] and high porosity [7, 8], however, there are also several disadvantages, as many of these techniques use solvents [5–8, 14–17] and allow only limited control over porosity [5–12], in particular several of the methods produce non-connected pore structures. Solid freeform techniques allow good control over the structure of the finished scaffold, however the size of features in the scaffold has a lower limit determined by the resolution of the printing technique [16, 17].

A further consideration is the incorporation of active molecules into the scaffold. In this way, drugs could be administered locally to the defect region. To improve the efficacy of this process the scaffold should be tailored to give a sustained release and a predictable

therapeutic response. Recent efforts have been focussed on the use of growth factors to induce and maintain differentiated cell function [18]. Scaffold fabrication techniques that use high temperatures or pressures may cause denaturing of these proteins and exclude their incorporation. Furthermore, the total porosity and average pore size have been shown to have a significant effect on the scaffold degradation rate and consequently on the release of the active molecules [19, 20].

This work describes a technique for the fabrication of polymeric scaffolds using a traditional solid porogen technique. The method builds on previous research by employing a regularly shaped porogen, pre-assembled into a chosen architecture. The larger pores in the final scaffold are directly determined by the spatial distribution of the porogen particles and the amount of uncontrolled porosity, with smaller pore sizes, can be tailored by changing the method of polymer impregnation to suit varied functions. The method allows good control over the scaffold morphology and the porogen pre-assembly techniques can be used to create a fully 3-dimensionally connected pore network, layered porosity or highly directional cylindrical pores in the final structure.

2. Materials

Commercial sugar spheres were kindly given by NP Pharm, France and were supplied in pre-sieved sets of five different size ranges, 200–300 μm, 355–500 μm, 500–650 μm, 650–710 μm and 710–850 μm. (greater than 92% of the spheres lie within the size range stated.) The sugar spheres consisted of a sucrose core surrounded by a native maize starch coating.

Polyglycolide (PGLA) was obtained from Alkermes, USA and a solution was made by adding 1 g of PGLA to 10 ml of acetone (obtained from Fisher Scientific, UK).

A two-part epoxy resin system, SpeciFix-20, was obtained from Struers, Germany and made up as per instructions, 7 parts resin to 1 part curing agent by weight.

3. Fabrication methods

3.1. Method 1

3.1.1. Fabrication of random packed sugar sphere compacts

Disc-shaped moulds were made from aluminium, the hole having diameter 15 mm and depth 5 mm. The moulds had no base and were placed on PTFE release film during the filling and drying stages of the manufacturing process. This mould design allowed the finished compacts to be pushed out easily from the moulds. To form the random compact, the sugar spheres were first spread over the bottom of a glass petri dish and sprayed with distilled water until their surfaces became moist and they started to clump together. This was due to the capillary forces between the spheres. The moistened spheres were then packed into the circular moulds and pushed down firmly with a flat-faced spatula, to create a relatively flat upper surface and to aid joining of the spheres at their contact points. The compacts were dried at room temperature for 24 h. During the drying process a bridge between the spheres is formed (Fig. 1) due to recrystallisation of dissolved sucrose as the water evaporates, creating an interconnected sphere network.

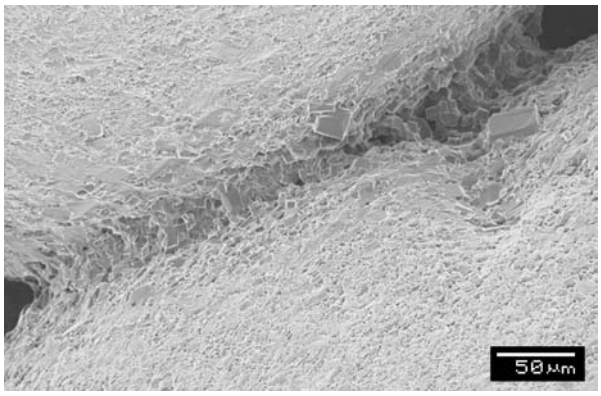

Figure 1 Scanning electron microscopy images of the fused region between two sugar spheres caused by recrystallisation of the sucrose.

3.1.2. Solution infiltration of polymer

To create one set of scaffolds, the sugar sphere compacts were impregnated with PGLA solution. The compacts were left in their moulds and placed in the bottom of plastic mounting cups only slightly larger than the moulds. These were placed in a chamber and evacuated (to a pressure of 200 mbar) to remove air from the sugar sphere compacts. The polymer solution was then infiltrated under a lower vacuum (pressure of 400 mbar), as the higher level of vacuum used previously caused the acetone to boil. After this step the scaffolds were maintained in a low vacuum for an hour to remove any air bubbles from the polymer solution. They were then left in a fume cupboard overnight to allow the acetone to fully evaporate. Once solidified, the scaffolds were removed from their moulds and placed into a beaker of water, stirred with a magnetic stirrer, for less than 12 h to wash out the sugar. Both this washing step, and subsequent dying, did not take long enough for any significant PGLA degradation to occur.

3.1.3. Resin impregnation

A second set of scaffolds was fabricated using a similar method, except an epoxy resin system was used in place of the PGLA solution. For this system the resin was infiltrated under the higher vacuum, as solvent evaporation was not a problem. Once set, the scaffolds were removed from their moulds and placed into a beaker of water to remove the sugar, as described earlier. The epoxy resin system itself is not biocompatible, however it provides a model system with which to demonstrate the application of this technique to reaction setting polymers. It is used to investigate the morphological differences between these scaffolds and those formed from a polymer solution.

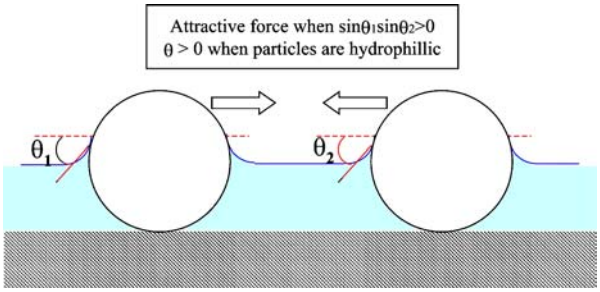

Figure 2 Lateral capillary force between immersed spheres.

3.2. Method 2

3.2.1. Fabrication of single layers of close-packed spheres

Two-dimensional arrangements of spheres can be formed in liquid layers by the capillary attraction between them (Fig. 2). The lateral capillary forces are caused by deformation of the liquid surface by the particles, and this deformation is related to the wetting properties of the particle surface. The larger the interfacial deflection, the greater the capillary force [21].

To form a layer of sugar spheres, a small amount of an ethanol/water mixture was spread on an acetate sheet and the sugar spheres were sprinkled over it. The acetate sheet was then agitated to draw the sugar spheres together. As the ethanol evaporated, the capillary forces between the spheres brought them into a close-packed arrangement. The small amount of water present in the mixture acted to moisten the surface of the spheres slightly and the spheres in the layer to stick together. Mixtures of ethanol and water were made up to different ratios, depending on the size of the sugar spheres. The correct ratio was determined to be the one which created a close-packed arrangement of spheres with a reasonable degree of connectivity, i.e. enough water to fuse the spheres in the layer together but not too much so that there was little or no distinction between one sphere and the next. In the final scaffold the fused areas create the dimensions of the connections between the pores. As the size of the sugar spheres increased, a greater percentage of water was required to form bridges between them, see Fig. 3. Once the solvent had fully evaporated and the spheres had fused together, the layers could be removed from the acetate sheet.

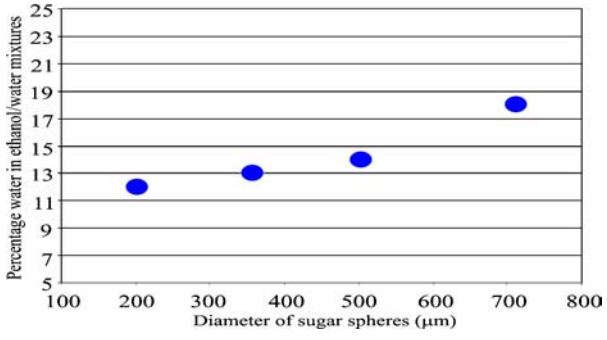

Figure 3 Variation of ethanol/water mixtures with size of sugar spheres. Points are plotted against the lower boundary of the size range of each set of sugar spheres.

3.2.2. Fabrication of multi-layered structures

Multi-layered scaffolds were formed by stacking the single layers on top of one another to form a 3D structure. A new layer was joined to the layer below by spraying the top of the lower layer with distilled water to moisten the surface. The upper layer was then rested on top and pressed down gently so as not to disrupt the individual layers. The joined layers were then sprayed a second time, to allow the water to infiltrate through the gaps in the upper layer and form a stronger bond between the layers. Subsequent layers were not added until those below were fully dried.

4. Analysis

4.1. X-ray microtomography

A desktop X-ray microtomograph (Skyscan 1072) was used as a non-destructive technique to image the internal structure of the scaffolds. A central section was cut from each of the scaffolds and imaged at a resolution of approximately 8 μm. Scans were performed at 100 kV with no filter. A step size of 0.45 °, exposure time of 1.9 s and an average of two frames were used. The shadow images were then reconstructed to form 2D slices and complete 3D representations of the scaffolds.

4.2. Image analysis

Two traditional stereology methods [22] were used to calculate the porosity of the resin impregnated scaffolds made using the randomly packed sugar sphere compacts. Both analyses used measurements taken from the 2D X-ray microtomography slices. Slices were chosen 50 or 100 μm apart, to give a representative set of five or six slices for each scaffold.

4.2.1. Line analysis

It can be shown that if a line is drawn through a 3D object, then the fraction of this line that intercepts a particular phase of the solid is equal to the volume fraction of that phase [22]. A similar derivation finds that the fraction of the phase found along a line drawn across a 2D plane through the solid is also equal to the volume fraction. In this analysis three lines were drawn across each slice, as shown in Fig. 4. It is not necessary to randomise the orientation of the lines to provide a true estimate of the volume fraction, however introducing a difference in orientation allowed the isotropy of the pore distribution to be checked. The proportion of solid polymer to pores was measured along each of these lines. An average for each slice was calculated and an overall average for each scaffold was obtained. This was then directly translated into a porosity volume fraction.

4.2.2. Area analysis

Image analysis software (Leica Qwin) was used to calculate the area percentage of solid material for each 2D slice. Each slice was manually thresholded to create a

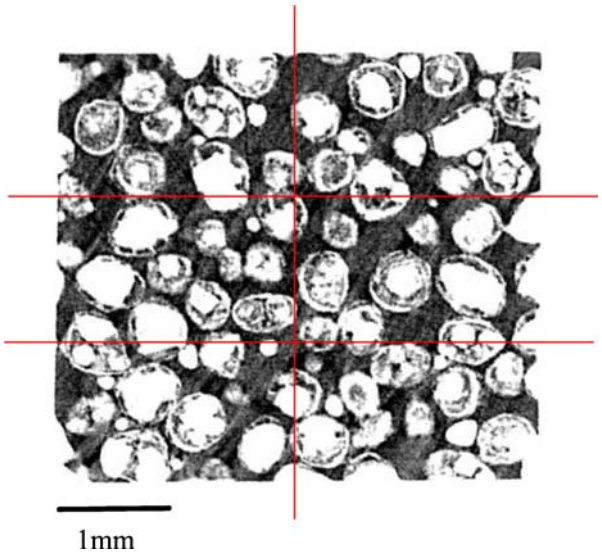

Figure 4 Position of 1D image analysis lines on the central section from a 2D X-ray tomography slice of a resin scaffold.

binary image. A measurement field was then created and the area percentage of solid material within that field was calculated. An average percentage was then calculated for each scaffold. In this analysis, the area percentage is equivalent to the volume fraction [22], and as before the orientation of the planes used in the analysis does not have to be randomised with respect to the whole structure. From the area fraction the solid volume fraction was obtained, and the scaffold porosity was calculated by subtracting the solid volume percentage from 100%.

5. Results

5.1. Sugar sphere structures

Reconstructed 2D and 3D X-ray microtomography images of a sugar sphere compact, a single close-packed layer and a multilayered structure are shown in Fig. 5. The hexagonal packing is clear to see in the single layer, while there is an obvious lack of order in the random compact. It is difficult to tell from the image of the multilayered structure if the two-dimensional order of the single layers has been extended fully to three dimensions.

5.2. PGLA scaffolds

The PGLA scaffolds, formed by the solvent impregnation technique, show both larger pores (diameter greater than 100 μm) with a morphology determined by the sugar spheres, and uncontrolled porosity (pore diameters less than 100 μm) caused by the movement of the acetone through the structure and the loss in volume of the PGLA/acetone phase as the solvent evaporated (Fig. 6).

5.3. Resin scaffolds

In the case of the resin scaffolds, the porosity was determined solely by the presence of the sugar spheres in the original compacts (Fig. 7). There is no longer any uncontrolled porosity and the morphology of the pores is the same throughout the scaffolds. The overall porosity of the resin scaffolds, as determined by the two different techniques, is shown in Fig. 8. The value of porosity remains largely constant at about 60% over the range of porogen sizes, with a slight drop for the largest sugar sphere size range used in these experiments.

5.4. Multi-layered structures

The X-ray tomography images of the multi-layered scaffold (Fig. 9) show that the close-packed arrangement of the sugar spheres did not extend to three dimensions. The close packed layers are still present, but these are generally separated by a layer of polymer. Moving sequentially through the 2D vertical slices showed that the porous layers were only connected at a few points.

6. Discussion

The use of sugar spheres as a solid porogen creates scaffolds consisting of pores with a regular spherical morphology. The creation of a network, in which the sugar spheres are fused together, prior to the infiltration of polymer, creates a high level of interconnectivity through the scaffold.

6.1. PGLA scaffolds

The use of a polymer solution leads to the formation of uncontrolled porosity within the scaffold. The

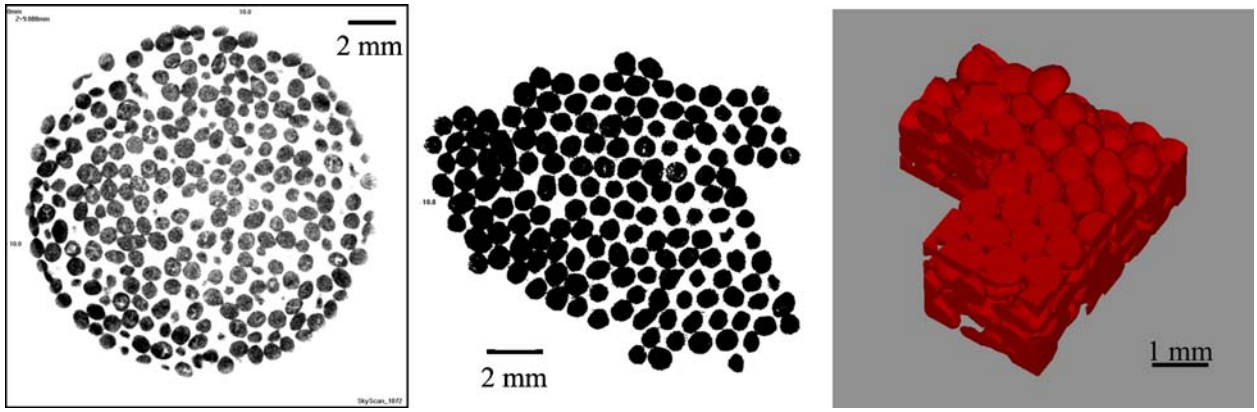

(a) (b) (c)

Figure 5 X-ray tomography images of sugar sphere structures, (a) 2D slice through a random compact, (b) 2D slice through a single close-packed layer, (c) 3D reconstruction of multilayers.

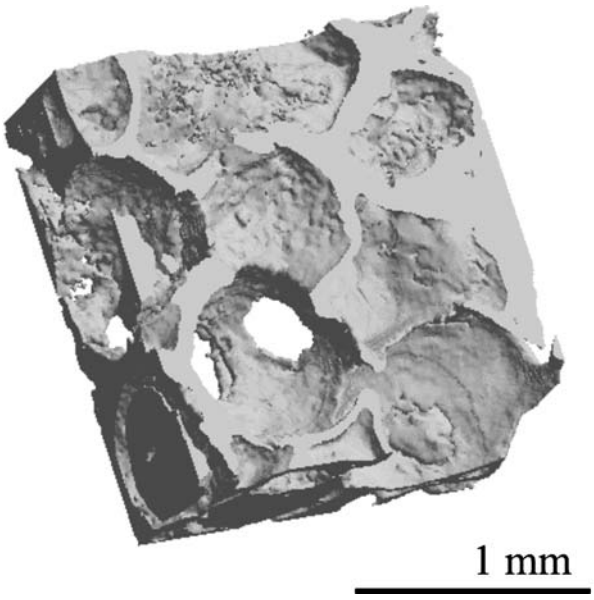

Figure 6 X-ray tomography 3D reconstruction of a scaffold made from PGLA (sugar sphere diameter 850–1000 μm).

dimensions of this porosity may be suitable for the promotion of cell proliferation and growth, while the network of interconnected, larger spherical pores provides a pathway of suitable dimensions for vascularisation throughout the scaffold. However, the presence of the uncontrolled porosity causes a lack of predictable mechanical properties and degradation behaviour. This can be overcome by using a system in which the polymer is infiltrated into the porogen network as a melt and then solidifies, or one in which the polymer solidifies through a reaction mechanism, as demonstrated by the resin scaffolds.

6.2. Resin scaffolds

The porosity value of about 60% obtained for these scaffolds is close to the theoretical value for dense randomly packed spheres. Random packing of spheres in three dimensions can give packing densities of 0.06 to 0.65. For random close-packed spheres a value of 0.64 is generally taken [23]. This theoretical value is calculated based on an infinite array of spheres. The system used in this work, however, is obviously finite, bounded by the mould. Therefore edge effects must be taken into consideration. As the size of the spheres increases to 710–850 μm the edge effects become more important. This causes the overall density of the packed spheres to decrease and leads to a similar decrease in the porosity of the final resin scaffolds. The porosity results for spheres up to 700 μm, however, show that this technique can be used to create scaffolds in which a constant value of porosity is maintained, while the dimensions of the individual pores change.

Along with affecting the flow of cells and nutrients through the scaffold, the pore dimensions will also affect the surface area of the scaffold and therefore, potentially, the rate of degradation. A simple calculation can be used to indicate how the surface area of the scaffold would be affected by the size of the sugar spheres, by considering the surface area of densely packed spheres.

The volume of a sphere is,

$$V_S = {}^4\!/_3 \pi r^3$$

So the number of spheres per unit volume is given by,

$$N_S = \frac{3\nu}{4\pi r^3}$$

where ν is the volume fraction of spheres (which in the case of scaffold manufacture would be equal to the porosity). The surface area of a sphere is,

$$A_S = 4\pi r^2$$

Combining these equations, the surface area per unit volume is found to be,

$$A = \frac{3\nu}{r}$$

i.e. the surface area will increase as the radius of the spheres decreases.

This result is an approximation and does not take into account the joins between the spheres. The true result would, therefore, be less than that obtained here. However, it demonstrates that this method of

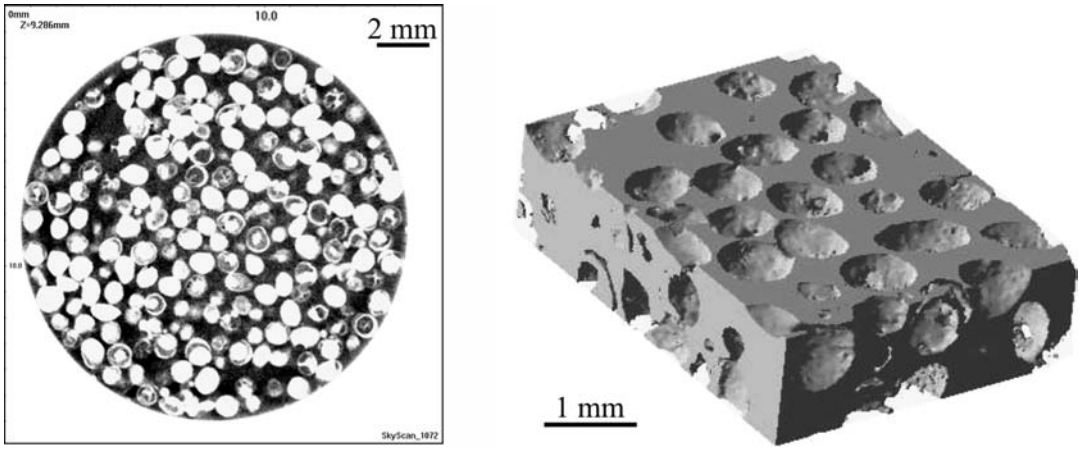

(a) (b)

Figure 7 X-ray tomography images of a resin scaffold (a) 2D slice (b) 3D reconstruction of central section of scaffold.

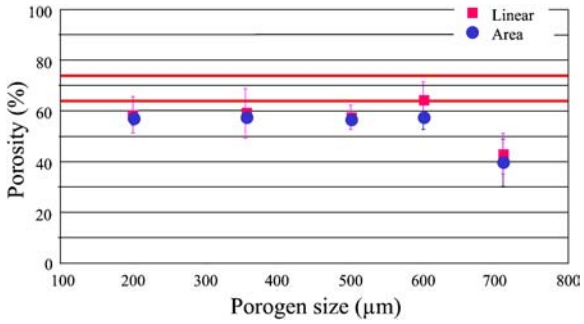

Figure 8 Porosity results from image analysis of resin scaffolds (bold lines indicate 64 and 74% porosity levels).

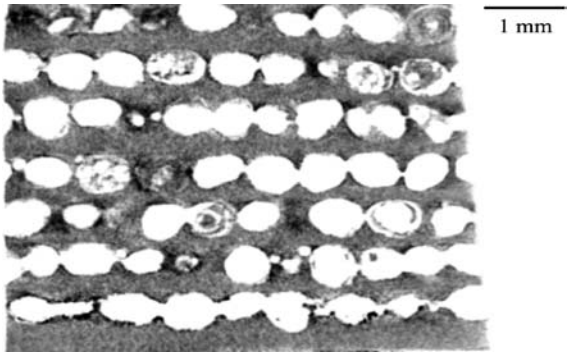

Figure 9 X-ray tomography 2D slice of a resin scaffold formed using a multi-layered sugar sphere structure.

scaffold fabrication could have important consequences for uses in tissue engineering and the delivery of active molecules, as it may be possible to control the rate of degradation and tortuosity of the scaffold without changing the overall level of porosity.

6.3. Multi-layered scaffolds

The architecture of the multi-layered scaffolds is significantly different from that of those formed from the randomly packed spheres. In the latter case, the porosity is isotropic, and it is therefore likely that the properties of the scaffolds, such as strength and degradation are also likely to be isotropic. In contrast the multi-layered scaffolds are anisotropic.

The porous layers are interconnected, but only at a few points over their area. This is primarily due to the fact that the majority of the sugar 'spheres' are not truly spherical and the spheres in one scaffold are of a range of sizes, therefore the natural roughness of the layers mean that they do not sit perfectly on top of one another.

The two-dimensional structure of these scaffolds may lead to interesting degradation and diffusion profiles, which could be used to tailor the release of drugs and biomolecules contained within the scaffold. An anisotropic structure may also be useful for generating different tissues types.

The results also demonstrate that it may be possible to create a fully close-packed 3D architecture. This would give a porosity of 74% (indicated on Fig. 8), in comparison to the figure of 60–64% created by the randomly packed sugar spheres. In order to achieve this structure the diameter of the sugar spheres would need to be more

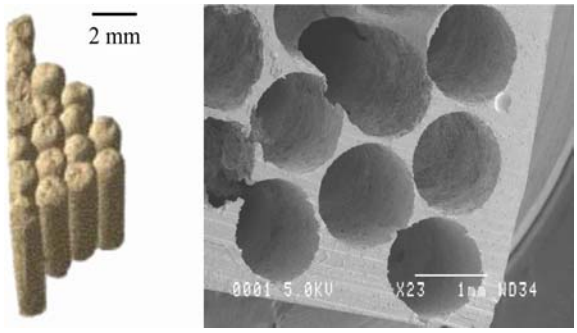

(a) (b)

Figure 10 (a) 3D X-ray microtomography reconstruction of an assembly of close-packed sugar strands (b) An SEM image of the resultant resin scaffold.

monodisperse in order to create contact points between all of the spheres in the layers.

7. Other architectures

The techniques outlined above can also be applied to create structures using close-packed sugar strands. Other groups have looked at the use of highly water soluble sugar fibres [24] to create highly porous interconnected scaffolds. In that work the fibres were randomly oriented and joins between them were created by localised areas of melting.

In this work, the method used to form the sugar sphere structures was also applied to sugar strands. The strands were arranged in a mould in which two sides were fixed at 60° to each other. They were then sprayed with distilled water to form a number of joins between the cylindrical sugar strands along their length (Fig. 10(a)). Due to irregularities in the commercial sugar strands, joins do not form along the entire length of the cylinders, but instead form at discrete points.

The resultant scaffold architecture (Fig. 10(b)) consists of partially interconnected cylindrical pores, once the sugar has been washed out. The degradation profile of these scaffolds and drug release rates from these structures are likely to be different again. The pore structure formed in the scaffold by the strands may be useful for the regeneration of highly directional biological tissues. Further porosity, making the scaffold more suitable for tissue engineering, may be created by combining both sugar strands and spheres in the same scaffold.

8. Conclusions

The use of a regularly shaped solid porogen has been used successfully to form polymeric scaffolds, in which the spatial distribution and dimensions of the pores can be changed without affecting the overall porosity of the scaffold. The method of pre-assembling the sugar spheres into random compacts creates a scaffold with a final porosity of about 60%, similar to the density of random close-packed spheres. Further, it has been demonstrated that decreasing the size of the sugar spheres may lead to an increase in the surface area of the scaffold, which may in turn increase the release rate of active ingredients held within the structure.

By impregnating the sugar compacts with polymers in different forms the degree of uncontrolled porosity with a smaller pore size (<100 μm diameter) can be tailored to a given requirement, while still defining the larger pores (>100 μm diameter) by the arrangement of the sugar spheres themselves.

Finally it has been demonstrated that a fully 3-dimensionally connected pore network, layered porosity or highly directional cylindrical pores in the final structure can be achieved through careful consideration of the geometry and arrangement of the porogen particles that are used. This will have major benefits it terms of tailoring the scaffold architecture to promote the growth of different tissue types and is also likely to affect the drug release profile from these structures.

Acknowledgment

We would like to thank the Pfizer Institute for Pharmaceutical Materials Science for funding this project.

References

1. S. YANG, K.-F. LEONG, Z. DU and C.-K. CHUA, *Tissue Eng.* **7** (2001) 679.
2. A. VATS, N. S. TOLLEY, J. M. POLAK and J. E. GOUGH, *Clin. Otolaryngol.* **28** (2003) 165.
3. A. C. JONES, B. MILTHORPE, H. AVERDUNK, A. LIMAYE, T. J. SENDEN, A. SAKELLARIOU, A. P. SHEPPARD, R. M. SOK, M. A. KNACKSTEDT, A. BRANDWOOD, D. ROHNER and D. W. HUTMACHER, *Biomater.* **25** (2004) 4947.
4. F. J. O'BRIEN, B. A. HARLEY, I. V. YANNAS and L. J. GIBSON, *ibid.* **26** (2005) 433.
5. Y. S. NAM and T. G. PARK, *ibid.* **20** (1999) 1783.
6. P. R. LAITY, P. M. GLOVER, A. BARRY and J. N. HAY, *Polymer* **42** (2001) 7701.
7. M. EPPLE and O. HERZBERG, *J. Mater. Chem.* **7** (1997) 1037.
8. V. P. SHASTRI, I. MARTIN and R. LANGER, *Proceedings of the National Academy of Sciences of the USA* **97** (2000) 1970.
9. Y. S. NAM, J. J. YOON and T. G. PARK, *J. Biomed. Mater. Res.* **53** (2000) 1.
10. M. E. GOMES, A. S. RIBEIRO, P. B. MALAFAYA, R. L. REIS and A. M. CUNHA, *Biomaterials* **22** (2001) 883.
11. A. I. COOPER *J. Mater. Chem.* **10** (2000) 207.
12. S. M. HOWDLE, M. S. WATSON, M. J. WHITAKER, V. K. POPOV, M. C. DAVIES, F. S. MANDEL, J. D. WANG and K. M. SHAKESHEFF, *Chemical Communications* (2001) 109.
13. L. GUAN and J. E. DAVIES, *J. Biomed. Mater. Res.* **71A** (2004) 480.
14. R. BUTLER, C. M. DAVIES and A. I. COOPER, *Adv. Mater.* **13** (2001) 1459.
15. H. ZHANG and A. I. COOPER, *Chem. Mater.* **14** (2002) 4017.
16. J. M. TABOAS, R. D. MADDOX, P. H. KREBSBACH and S. J. HOLLISTER, *Biomater.* **24** (2003) 181.
17. W.-Y. YEONG, C.-K. CHUA, K.-F. LEONG and M. CHANDRASEKARAN, *Trends in Biotechnology* **22** (2004) 643.
18. V. LUGINBUEHL, L. MEINEL, H. P. MERKLE and B. GANDER, *Eur. J. Pharm. Biopharm.* **58** (2004) 197.
19. K. ZYGOURAKIS and P. A. MARKENSCOFF, *Biomater.* **17** (1996) 125.
20. J. BRAUNECKER, M. BABA, G. E. MILROY and R. E. CAMERON, *Int. J. Pharm.* **282** (2004) 19.
21. P. A. KRALCHEVSKY, N. D. DENKOV, V. N. PAUNOV, O. D. VELEV, I. B. IVANOV, H. YOSHIMURA and K. NAGAYAMA, *J. Phys. Condens. Matter* **6** (1994) A395.
22. J. E. HILLIARD, in "Quantitative Microscopy", edited by R.T. DeHoff and F.N. Rhines (McGraw Hill, 1968) p. 45.
23. *Nature* **239** (1972) 488.
24. R. FILMON, N. RETAILLEAU-GABORIT, F. GRIZON, M. GALLOYER, C. CINCU, M. F. BASLE and D. CHAPPARD, *J. Biomater. Sci. Polymer Edn.* **13** (2002) 1105.

Received 29 June
and accepted 27 July 2005